

Andreev reflection mediated Δ_T noise

Tusaradri Mohapatra and Colin Benjamin

*School of Physical Sciences, National Institute of Science Education & Research, Jatni-752050, India,
Homi Bhabha National Institute, Training School Complex, Anushaktinagar, Mumbai 400094, India*

Quantum noise has been extensively utilized to investigate various aspects of quantum transport, such as current-current correlations and wave-particle duality. A recent focus in this field is on Δ_T quantum noise, which arises because of a finite temperature difference at vanishing charge current. This paper explores the characterization of Δ_T noise auto-correlation alongside the shot noise and thermal-noise contributions in a 1D metal/insulator/superconductor junction. We consider a finite temperature gradient with zero applied bias for reservoirs at comparable temperatures. Andreev reflection enhances the Δ_T noise in a metal-insulator-superconductor junction in contrast to a metal-insulator-metal junction in the transparent limit. Unlike quantum noise for which shot-noise dominates thermal-noise at large bias voltages and finite barrier strength, Δ_T thermal-noise is always higher than Δ_T shot-noise. Thus, a general bound that is independent of barrier strength is established. This investigation sheds light on the distinct behavior of Δ_T noise, alongside the ratio of shot-noise to thermal-noise contributions, offering valuable insights into the intricate interplay between finite temperature gradient, barrier strength, and Andreev reflection.

I. INTRODUCTION

The transport characteristics of mesoscopic devices can be effectively studied by analyzing quantum noise, which provides valuable insights into various aspects, including distinguishing wave-particle duality and offering a deeper understanding of quantum statistics [1, 2, 4]. Recently, Δ_T noise has garnered significant interest from both theoretical [5–7] and experimental measurements, as it has been observed across conductors using atomic-scale molecular junction [9], seen in quantum circuits [10], and also in metallic tunnel junctions [11]. Charge Δ_T noise arises in non-equilibrium systems due to a finite temperature gradient [9]. Unlike quantum noise, Δ_T noise can occur with no net charge current in systems with two reservoirs having a temperature gradient. Charge Δ_T noise adheres to the general bound as mentioned in Ref. [7]; which indicates that the Δ_T thermal-noise ($\Delta_{T\text{th}}$) is always higher than or equal to Δ_T shot-noise ($\Delta_{T\text{sh}}$), i.e., $\Delta_{T\text{sh}}/\Delta_{T\text{th}} \leq 1$.

Experimentally, Δ_T shot-noise can be measured after subtracting the Δ_T thermal-noise from total Δ_T noise [9]. Sometimes, in experimental setups, unintentional temperature differences can lead to abrupt noise that might be mistaken for noise originating from the charge carriers' interactions or other subtle effects, see [9]. It can be effectively examined using Δ_T noise. The versatility of Δ_T noise measurement makes it an effective tool for investigating and understanding such occurrences, as it is not bound by specific design constraints [10]. Furthermore, Δ_T noise measurement is not restricted to a particular temperature range, allowing its application to conductors of varying sizes down to the atomic scale [9, 10].

In this paper, Δ_T noise in a 1D metal/insulator/superconductor (NIS) junction is calculated so as to understand the effect of Andreev reflection in such junction with a temperature gradient [13]. We consider finite temperature gradient configuration at zero voltage bias (given in subsections II B) for contacts with comparable temperatures. Total Δ_T noise in NIS junction is always positive due to the positive Δ_T shot-noise and the positive Δ_T thermal-noise contributions. Andreev reflection enhances Δ_T noise in NIS junction compared to that

in a metal/insulator/metal (NIN) junction. When the barrier strength approaches zero in the transparent limit, the Δ_T noise in a NIS junction is twice the magnitude of the Δ_T noise in a NIN junction due to perfect Andreev reflection. It is due to the finite Δ_T thermal-noise in the transparent limit, which is the dominant contribution. However, in the tunnel limit, i.e., for large barrier strength, the Δ_T noise in the NIS junction tends toward the same value as the Δ_T noise in the NIN junction. The Δ_T noise in a NIN junction aligns with the Δ_T noise in a metal/spin-flipper/metal junction, in absence of spin-flip scattering akin to a NIN junction, as shown in Ref. [17]. It acts as a consistency check of our results. In the case of quantum noise, quantum shot-noise dominates quantum thermal-noise at large bias voltage, and quantum thermal-noise dominates at high-temperature bias. On the contrary, Δ_T thermal-noise always dominates, obeying the general bound. Overall, our study highlights the sensitivity of Δ_T noise to changes in barrier strength and the importance of Andreev reflection.

The paper follows this structure: section II presents an overview of quantum transport in a NIS junction, focusing on wave functions and boundary conditions to calculate the scattering amplitudes. We then derive finite temperature gradient quantum noise and discuss Δ_T noise. Section III discusses the characteristics of Δ_T noise, including the ratio of $\Delta_{T\text{sh}}/\Delta_{T\text{th}}$ to examine the impact of Andreev reflection. In section IV, we analyze the Δ_T shot-noise and Δ_T thermal-noise contributions to Δ_T noise and investigate the barrier strength dependence in the transparent and tunnel limit. In section V, we discuss our work's experimental realization and conclusion. The theoretical derivation of current is given in Appendix A. Appendix B contains the calculation of quantum noise in both NIS and NIN junctions. Appendices C 1 and C 2 contain derivation of the thermovoltage required to calculate the Δ_T noise and derivation of both Δ_T shot-noise and Δ_T thermal-noise, respectively.

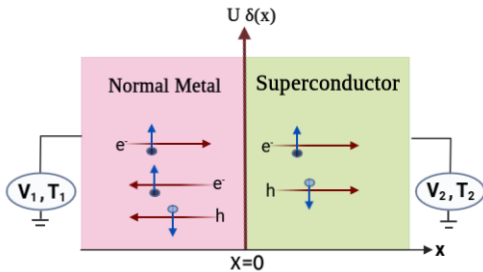


Figure 1. Schematic of 1D normal metal/insulator/superconductor junction (NIS) with a δ potential barrier located at the interface of NIS junction ($x = 0$).

II. THEORY

The Hamiltonian for a NIS junction, using the Bogoliubov-de Gennes (BDG) formalism as described in Ref. [14], can be expressed as follows:

$$\mathcal{H} = \begin{pmatrix} H_0(\mathbf{k}) & \Delta_0 \Theta(x) \\ \Delta_0^\dagger \Theta(x) & -H_0^*(-\mathbf{k}) \end{pmatrix}, \quad (1)$$

with $\Theta(x)$ is Heaviside theta function, Δ_0 is the superconducting gap [15], and k_B is Boltzmann constant. $H_0(\mathbf{k}) = -\frac{\hbar^2 \mathbf{k}^2}{2m^2} + U\delta(x) - E_F$, where U represents the barrier potential at the interface, E_F is the Fermi energy, and m^* is the mass of the electron.

The wave functions in normal metal (N) and superconductor (S) regions, for an electron incident from normal metal N are given as (see, Fig. 1),

$$\begin{aligned} \psi_N(x) &= \begin{pmatrix} 1 \\ 0 \end{pmatrix} (e^{ik_e x} + b e^{-ik_e x}) + a \begin{pmatrix} 0 \\ 1 \end{pmatrix} e^{-ik_h x}, \text{ for } x < 0, \\ \psi_S(x) &= c \begin{pmatrix} u \\ v \end{pmatrix} e^{ik_e^s x} + d \begin{pmatrix} v \\ u \end{pmatrix} e^{-ik_h^s x}, \text{ for } x > 0, \end{aligned} \quad (2)$$

where $k_{e,h}$ are wave-vectors in normal metal for electron and hole, i.e., $k_{e,h} = \sqrt{\frac{2m^*}{\hbar^2}(E_F \pm E)}$, wherein E is the excitation energy of the electron and $k_{e,h}^s$ are the wave-vectors in the superconductor for electron-like and hole-like quasi-particles, i.e., $k_{e,h}^s = \sqrt{\frac{2m^*}{\hbar^2}(E_F \pm \sqrt{E^2 - \Delta_0^2})}$. The coherence factors for energy E above the superconducting gap Δ_0 are $u(v) = \left[\frac{1}{2} \left\{ 1 \pm \frac{\sqrt{E^2 - \Delta_0^2}}{E} \right\} \right]^{1/2}$. In a NIS junction, an incident electron on the interface undergoes two possible reflections: normal reflection, where it is reflected as an electron, or Andreev reflection, where it is reflected as a hole. The Andreev reflection is characterized by the amplitude $a = s_{11}^{he}$, while the normal reflection is denoted by the amplitude $b = s_{11}^{ee}$. Furthermore, there are two transmission amplitudes: $c = s_{21}^{ee}$ represents the transmission amplitude of an electron transmitted as an electron, and $d = s_{21}^{he}$ represents the transmission

amplitude of an electron transmitted as a hole, and their respective probabilities are defined as $A = (k_h/k_e)|a|^2$, $B = |b|^2$, $C = (k_e^s/k_e)(|u|^2 - |v|^2)|c|^2$ and $D = (k_h^s/k_e)(|u|^2 - |v|^2)|d|^2$ [14]. The prefactors $(|u|^2 - |v|^2)$, (k_h/k_e) , and $(k_{e,h}^s/k_e)$ arise from the need to conserve the probability current, see Ref. [14]. The scattering amplitude $s_{ik}^{\rho\Gamma}$ describes the behavior of a particle with type Γ (either electron e or hole h) incident from contact k (either N or S) that is either reflected or transmitted to contact i (either N or S) as a particle of type ρ (either electron e or hole h).

The boundary conditions for electron incident from N to S , at the interface $x = 0$ (see, Fig 1) in a NIS junction are,

$$\begin{aligned} \psi_N(x = 0) &= \psi_S(x = 0), \\ \frac{d\psi_S(x = 0)}{dx} - \frac{d\psi_N(x = 0)}{dx} &= \frac{2m^* U}{\hbar^2} \psi_N(x = 0). \end{aligned} \quad (3)$$

Incorporating Eq. (2) into Eq. (3), we get scattering amplitudes with barrier strength characterized by dimensionless parameters $Z = m^* U / (\hbar^2 k_F)$, where $k_F = \sqrt{\frac{2m^* E_F}{\hbar^2}}$ is Fermi wave vector.

In the following subsections, we compare the current, quantum noise, and Δ_T noise in a NIS junction as shown in Fig 1 with a NIN junction.

A. Current and quantum noise

For our chosen setup depicted in Fig. 1, the average current in contact i is [2, 16],

$$\langle I_i^{NIS} \rangle = \frac{e}{h} \sum_{\substack{k, l \in \{1, 2\}; \\ \rho, \Gamma, \eta \in \{e, h\}}} sgn(\rho) \int_{-\infty}^{\infty} dE A_{k\Gamma;l\eta}(i\rho, E) \langle a_{k\Gamma}^\dagger a_{l\eta} \rangle, \quad (4)$$

where $sgn(\rho) = +1$ for electron and -1 for hole. $A_{k\Gamma;l\eta}(i\rho, E) = \delta_{ik} \delta_{il} \delta_{\rho\Gamma} \delta_{\rho\eta} - s_{ik}^{\rho\Gamma} s_{il}^{\rho\eta}$, with i, k and l indices label normal metal, i.e., 1 and superconductor, i.e., 2, and ρ, Γ, η denote electron or hole (see, Appendix A). $a_{k\Gamma}^\dagger$ ($a_{l\eta}$) are electron creation (annihilation) operators of electron or hole in contact k (l). The expectation value of the product of the fermionic creation and annihilation operators [2] simplifies to $\langle a_{k\Gamma}^\dagger a_{l\eta} \rangle = \delta_{kl} \delta_{\Gamma\eta} f_{k\Gamma}$, $f_{k\Gamma}(E) = \left[1 + e^{\frac{E + sgn(\Gamma)V_k}{k_B T_k}} \right]^{-1}$ being Fermi function in contact k and particle $\Gamma \in \{e, h\}$, with $sgn(\Gamma) = +$ for electron and $-$ for hole. T_k and V_k are temperature and applied voltage bias in contact k . By simplifying Eq. (4), the average current [18] in normal metal N in a NIS junction can be written as,

$$\begin{aligned} \langle I_1^{NIS} \rangle &= \frac{e}{h} \sum_{\substack{k, l \in \{1, 2\}, \\ \rho, \Gamma, \eta \in \{e, h\}}} sgn(\rho) \int_{-\infty}^{\infty} dE A_{k\Gamma;l\eta}(1\rho, E) \langle a_{k\Gamma}^\dagger(E) a_{l\eta}(E) \rangle \\ &= \frac{2e}{h} \int_{-\infty}^{\infty} (1 + A - B)(f_{1e} - f_{2e}) dE \\ &= \frac{2e}{h} \int_{-\infty}^{\infty} F_I^{NIS}(f_{1e} - f_{2e}) dE, \end{aligned} \quad (5)$$

where $F_I^{NIS} = 1 + A - B$. For a NIN junction, in the absence of Andreev reflection, the average current is defined as $\langle I_1^{NIN} \rangle = \frac{e}{h} \int_{-\infty}^{\infty} F_I^{NIN} (f_{1e} - f_{2e}) dE$, with $F_I^{NIN} = 1 - B = \mathcal{T}$, where \mathcal{T} is the transmission probability, see Appendix A. Quantum noise auto (cross) correlation defines the current-current correlation in the normal metal N (or cross correlation between normal metal N and superconductor S). In general, quantum noise correlations [1] between current in contacts p and q at time t and t' can be written as $S_{pq}^{xy}(t - t') \equiv \langle \Delta I_p^x(t) \Delta I_q^y(t') + \Delta I_q^y(t') \Delta I_p^x(t) \rangle$, where $\Delta I_p^x(t) = I_p^x(t) - \langle I_p^x(t) \rangle$, and $\{x, y\} \in \{e, h\}$. Fourier transformation of the quantum noise yields the quantum noise power, which can be expressed in terms of frequency as $\delta(\omega + \bar{\omega}) S_{pq}^{xy}(\omega) \equiv \frac{1}{2\pi} \langle \Delta I_p^x(\omega) \Delta I_q^y(\bar{\omega}) + \Delta I_q^y(\bar{\omega}) \Delta I_p^x(\omega) \rangle$. In general, the expression for zero frequency noise auto-correlation ($p = q = 1$) in NIS junction [16, 19] is,

$$\begin{aligned} S_{11}^{NIS}(\omega = 0) &= S_{11}^{sa}(\omega = 0) + S_{11}^{op}(\omega = 0) = \sum_{x \in \{e, h\}} S_{11}^{xx}(\omega = 0) + \sum_{\substack{y, x \in \{e, h\}, \\ x \neq y}} S_{11}^{xy}(\omega = 0) \\ &= (S_{11}^{ee}(\omega = 0) + S_{11}^{hh}(\omega = 0)) + (S_{11}^{eh}(\omega = 0) + S_{11}^{he}(\omega = 0)), \end{aligned}$$

where noise auto-correlation for same particles (S_{11}^{sa}) and noise auto-correlation for different particles (S_{11}^{op}) are defined as:

$$\begin{aligned} S_{11}^{sa} &= \frac{2e^2}{h} \int \sum_{\substack{k, l \in \{1, 2\}, \\ x, y, \Gamma, \eta \in \{e, h\}}} A_{k, \Gamma; l, \eta}(1x, E) A_{l, \eta; k, \Gamma}(1x, E) f_{k\Gamma}(E) [1 - f_{l\eta}(E)] dE, \\ S_{11}^{op} &= -\frac{2e^2}{h} \int \sum_{\substack{k, l \in \{1, 2\}, \\ x, y, \Gamma, \eta \in \{e, h\}, x \neq y}} A_{k, \Gamma; l, \eta}(1x, E) A_{l, \eta; k, \Gamma}(1y, E) f_{k\Gamma}(E) [1 - f_{l\eta}(E)] dE. \end{aligned} \quad (6)$$

The total quantum noise auto-correlation can be written as:

$$\begin{aligned} S_{11}^{NIS}(\omega = 0) &= \frac{2e^2}{h} \int \sum_{\substack{k, l \in \{1, 2\}, \\ x, y, \Gamma, \eta \in \{e, h\}}} sgn(x) sgn(y) A_{k, \Gamma; l, \eta}(ix, E) A_{l, \eta; k, \Gamma}(jy, E) f_{k\Gamma}(E) [1 - f_{l\eta}(E)] dE \\ \text{and } S_{11}^{NIS} &= \frac{4e^2}{h} \left[\int_{-\infty}^{\infty} F_{11th}^{NIS} \{f_{1e}(1 - f_{1e}) + f_{2e}(1 - f_{2e})\} dE + \int_{-\infty}^{\infty} F_{11sh}^{NIS} (f_{1e} - f_{2e})^2 dE \right] = S_{11th}^{NIS} + S_{11sh}^{NIS}, \end{aligned} \quad (7)$$

where $sgn(e) = +1$ for electron and $sgn(e) = -1$ for hole. The detailed derivation of the scattering terms $F_{11th}^{NIS} = 1 + A - B$, and $F_{11sh}^{NIS} = A(1 - A) + B(1 - B) + 2AB$ with A being the Andreev reflection probability and B the normal reflection probability are given in Appendix B. For a NIN junction, scattering terms for thermal-noise (S_{11th}^{NIN}) and shot-noise (S_{11sh}^{NIN}) auto-correlation are $F_{11th}^{NIN} = 1 - B = \mathcal{T}$, and $F_{11sh}^{NIN} = \mathcal{T}(1 - \mathcal{T})$, respectively.

In Eq. (7), S_{11th}^{η} is thermal-noise, and S_{11sh}^{η} is the shot-noise contributions to quantum noise auto-correlation S_{11}^{η} , where $\eta \in \{NIS, NIN\}$. The scattering terms, F_{11sh}^{η} and F_{11th}^{η} consist of reflection and transmission probabilities for shot-noise (S_{11sh}^{η}) and thermal-noise (S_{11th}^{η}) contributions respectively, such that for $\eta = NIS$, it depends on normal reflection and Andreev reflection probabilities in NIS junction and for $\eta = NIN$, it depends on the normal transmission probability in a NIN junction. The detailed calculations of quantum shot-noise (see, Eq. (B5)) and quantum thermal-noise (see, Eq. (B6)) are provided in Appendix B.

B. Δ_T noise

The noise arising due to a finite temperature difference at vanishing current is commonly referred to as Δ_T noise, as de-

scribed in previous studies [5–10]. Δ_T noise auto-correlation can be calculated from quantum noise auto-correlation S_{11} given in Eq. (7) for vanishing charge current by expanding the Fermi functions in a power series of temperature difference with normalized average temperature, i.e., $\frac{\Delta T}{2\bar{T}}$, where temperature difference $\Delta T = T_1 - T_2$ and average temperature $\bar{T} = (T_1 + T_2)/2$. The Δ_T noise is calculated in Appendix C2. The two contributions to Δ_T noise, similar to quantum noise are the Δ_T thermal-noise contribution (Δ_{Tth}) and Δ_T shot-noise contribution (Δ_{Tsh}), i.e., $\Delta_T = \Delta_{Tth} + \Delta_{Tsh}$. Vanishing charge current is achieved by imposing the zero charge current condition (i.e., $I_1 = 0$), regardless of voltage bias configuration with finite temperature gradient [8], given in Appendix C1.

In Fig. 2, we illustrate our chosen setup of reservoirs at comparable temperatures to study the Δ_T noise in a NIS junction. Here, we take the temperature in contact $k \in \{1, 2\}$ as T_k , where contact 1 represents the normal metal with temperature

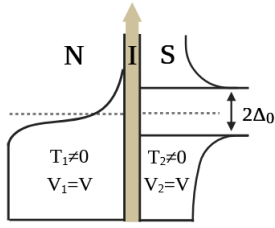


Figure 2. Schematics of a 1D NIS junction to measure Δ_T noise. Temperature difference: $T_1 - T_2 <$ average temperature: $(T_1 + T_2)/2$, with zero voltage bias ($\Delta V = 0$).

T_1 and contact 2 represents the superconductor with temperature T_2 such that $T_1 > T_2$. The average temperature across both contacts, denoted by \bar{T} , is calculated as $(T_1 + T_2)/2$. This average temperature \bar{T} is always greater than the temperature difference between the two contacts ($\Delta T = T_1 - T_2$). For zero voltage bias case, voltages in N and in S are same, i.e., $V_1 = V_2 = V$, see Fig. 2. Thermovoltage (V_{th}) refers to the applied voltage bias required to achieve zero net charge current flow, i.e., $I_1 = 0$ [7]. Herein, we simplify the Δ_T noise by expanding the Fermi functions in a power series of the temperature gradient, normalized by the average temperature ($\frac{\Delta T}{2\bar{T}}$), see Eqs. (C4) and (C6). For zero applied bias ($V_1 = V_2 = V$), Fermi distribution functions for electron (hole) in N is $f_{1q}(E \pm V) = \left[1 + e^{\frac{E \pm V}{k_B T_1}}\right]^{-1}$, where + is for $q = \text{electron}$, and - is for $q = \text{hole}$. Fermi function for electron-like (and hole-like) quasiparticle in S is $f_{2q}(E \pm V) = \left[1 + e^{\frac{E \pm V}{k_B T_2}}\right]^{-1}$ where + is for $q = \text{electron-like quasiparticle}$, and - is for $q = \text{hole-like quasiparticle}$.

The Fermi functions in current (see, Eq. (5)) and quantum noise (see, Eq. (7)) can be rewritten in terms of temperature difference and average temperature, such as $f_{1e}(T_1) = f_1(\bar{T} + \Delta T/2)$ and $f_{2e}(T_2) = f_2(\bar{T} - \Delta T/2)$.

The Fermi functions occurring in the average current I_1 can be expanded in power series of $\frac{\Delta T}{2\bar{T}}$ as $f_{1e} - f_{2e} = 2k_B \bar{T} \frac{\partial f(E)}{\partial k_B \bar{T}} \left(\frac{\Delta T}{2\bar{T}}\right)$, where $f(E) = 1/(1 + e^{\frac{E}{k_B T}})$. The full expanded form with contributions from $\left(\frac{\Delta T}{2\bar{T}}\right)^3$ is given in Eq. (C1) of Appendix A. The average current can be calculated numerically, using this Fermi function expansion, and then by equating $I_1 = 0$, we get the thermovoltage (V_{th}). The detailed derivation of thermovoltage (V_{th}) required to calculate Δ_T noise is given in Appendix C1.

Similarly, we expand the Fermi functions in quantum S_{11sh} shot and S_{11th} thermal-noise (see, Eqs. (B5) and (B6) in Appendix B) in power series of $\frac{\Delta T}{2\bar{T}}$, and the detailed derivation for Fermi function expansions are given in Eqs. (C4) and (C6) of Appendix C2. Δ_{Tsh} and Δ_{Tth} noise can be calculated numerically using the Fermi function expansion.

Δ_T^η shot-noise (Δ_{Tsh}^η) is calculated from quantum shot-noise S_{11sh}^η (see, Eq. (7)) numerically, by replacing the thermovolt-

age (V_{th}) (which ensures the vanishing charge current condition) in the voltage bias V , and taking the limit $\frac{\Delta T}{2\bar{T}} \ll 1$, Δ_{Tsh}^η noise is given as,

$$\Delta_{Tsh}^\eta = \frac{4e^2}{h} \int_{-\infty}^{\infty} F_{11sh}^\eta \left\{ 4 \left(k_B \bar{T} \frac{\partial f(E)}{\partial k_B \bar{T}} \right)^2 \left(\frac{\Delta T}{2\bar{T}} \right)^2 \right\} dE, \quad (8)$$

where $\eta = \{NIS, NIN\}$, and the Fermi function $f(E) = \left[1 + e^{\frac{E}{k_B \bar{T}}}\right]^{-1}$, see Appendix C2 for the full expanded form of Δ_{Tsh}^η noise with contributions from $\left(\frac{\Delta T}{2\bar{T}}\right)^4$ terms also. The scattering term F_{11sh}^η is function of Andreev and normal reflection probabilities for a NIS junction, with $F_{11sh}^{NIS} = A(1 - A) + B(1 - B) + 2AB$ (see, Eq. (B5)), while for a NIN junction ($\Delta_0 = 0$), $F_{11sh}^{NIN} = \mathcal{T}(1 - \mathcal{T})$ (see, Eq. (B7)).

Δ_T^η thermal-noise noise (Δ_{Tth}^η) is calculated numerically from quantum noise S_{11th}^η (see, Eq. (7)). Imposing vanishing charge current condition, and replacing the thermovoltage (V_{th}) in the voltage, and taking the limit $\frac{\Delta T}{2\bar{T}} \ll 1$, Δ_{Tth}^η noise can be derived to be,

$$\Delta_{Tth}^\eta = -\frac{4e^2}{h} \int_{-\infty}^{\infty} F_{11th}^\eta \left[2 \frac{\partial f(E)}{\partial E} (k_B \bar{T}) + (k_B \bar{T})^2 \left\{ \frac{\partial}{\partial E} \left(\frac{\partial^2 f(E)}{\partial (k_B \bar{T})^2} \right) \right. \right. \right. \\ \left. \left. \left. k_B \bar{T} + \frac{\partial}{\partial E} \left(2 \frac{\partial f(E)}{\partial k_B \bar{T}} \right) \right\} \left(\frac{\Delta T}{2\bar{T}} \right)^2 \right] dE, \quad (9)$$

see Appendix C2, for the full expanded form of Δ_{Tth}^η noise with contributions from $\left(\frac{\Delta T}{2\bar{T}}\right)^4$ terms also. The scattering term F_{11th}^η is a function of Andreev and normal reflection probabilities for a NIS junction, with $F_{11th}^{NIS} = 1 + A - B$ (see, Eq. (B6)), while for a NIN junction ($\Delta_0 = 0$), $F_{11th}^{NIN} = \mathcal{T}$ (see, Eq. (B7)). In the subsequent section, we discuss the characteristics of Δ_T noise in a NIS junction and compare it with a NIN junction.

III. RESULTS AND DISCUSSION

This section elaborates on the characteristics of Δ_T^η noise with finite temperature gradient in our chosen setup of reservoirs at comparable temperatures (see Fig. 1). We consider the superconducting material such as niobium (Nb) with Fermi energy $E_F = 100\Delta_0$, where $\Delta_0 = 1.39\text{meV}$. We plot Δ_T^η noise along with the ratio of Δ_T^η shot noise to Δ_T^η thermal-noise contributions, i.e., $\Delta_{Tsh}^\eta/\Delta_{Tth}^\eta$ in NIS as well as NIN junctions.

In Fig. 3, we show total Δ_T^η noise and $\Delta_{Tsh}^\eta/\Delta_{Tth}^\eta$ ratio as function of the barrier strength Z . We find that Δ_T^η noise remains finite in the transparent limit for both NIS and NIN junctions. In the transparent limit, Δ_T^{NIS} noise is double that of Δ_T^{NIN} noise solely due to contribution from perfect Andreev reflection in a NIS junction. However, in the tunnel limit, as Andreev reflection probability vanishes, Δ_T^{NIS} noise is the same as Δ_T^{NIN} noise, see Fig. 3(a).

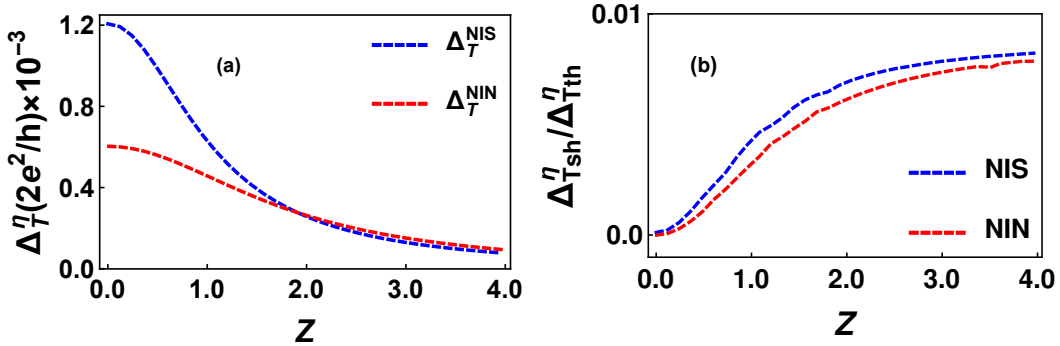


Figure 3. (a) Total Δ_T^η noise, and (b) ratio $\Delta_T^\eta_{Tsh}/\Delta_T^\eta_{Tth}$ vs. Z , with $\frac{\Delta T}{2T} = 0.14$, where $\eta = NIS$, (blue, dashed) NIN (red, dashed).

Additionally, we find that Δ_T^η noise adheres to the general bound, i.e., Δ_{Tth}^η noise is always greater than Δ_{Tsh}^η noise for both NIS and NIN junctions, see Fig. 3(b). In the transparent limit, the ratio $\Delta_{Tsh}^\eta/\Delta_{Tth}^\eta$ tends to zero for both NIS and NIN junctions, due to vanishing Δ_{Tsh}^η shot-noise. As the barrier strength increases, the ratio $\Delta_{Tsh}^\eta/\Delta_{Tth}^\eta$ also increases. Notably, in the tunnel limit, the $\Delta_{Tsh}^\eta/\Delta_{Tth}^\eta$ ratio tends toward a finite value for both NIS and NIN junctions, albeit with a higher magnitude for NIS junction compared to NIN junction.

In the transparent limit, the ratio of the scattering factors $F_{11sh}^{NIS}/F_{11th}^{NIS} \rightarrow 0$ as $F_{11sh}^{NIS} = A(1-A) + B(1-B) + 2AB$ vanishes due to perfect Andreev reflection ($A \rightarrow 1$) and $B \rightarrow 0$ for energy below the superconducting gap ($E < \Delta_0$). However, it vanishes for energy above the superconducting gap ($E > \Delta_0$) due to the absence of both Andreev and normal reflection ($A, B \rightarrow 0$). Conversely, in the tunnel limit, $F_{11sh}^{NIS}/F_{11th}^{NIS} \rightarrow 2$ for energy below the superconducting gap, reflecting the double shot-noise in the Fano factor, i.e., $S_{11sh}/(2eI_1) = 2$, and $F_{11sh}^{NIS}/F_{11th}^{NIS}$ tends to 1 for energy above the superconducting gap where there is no Andreev reflection [20].

For Δ_T^{NIS} noise, in the transparent limit ($Z \rightarrow 0$), the ratio $\Delta_{Tsh}^{NIS}/\Delta_{Tth}^{NIS} \rightarrow 0$ due to the vanishing Δ_{Tsh}^{NIS} , which depends on the scattering term F_{11sh}^{NIS} , see Eq. (8). In the tunnel limit, both Δ_{Tsh}^{NIS} and Δ_{Tth}^{NIS} noise vanish, but Δ_{Tsh}^{NIS} noise diminishes at a higher rate than Δ_{Tth}^{NIS} noise, solely due to the difference in dependence of temperature gradient (ΔT) in Δ_{Tsh}^{NIS} and Δ_{Tth}^{NIS} noise. For example, the first term in Δ_{Tth}^{NIS} thermal-noise shows \bar{T} dependence, which dominates the second term consisting of $(\Delta T)^2$ (see, Eq. (9)), while in the case of Δ_{Tsh}^{NIS} shot-noise, it shows $(\Delta T)^2$ dependence (see, Eq. (8)). Hence, the ratio $\Delta_{Tsh}^{NIS}/\Delta_{Tth}^{NIS}$ does not tend to 1 but tends to a small finite value, see, Fig. 3(b).

Our result for Δ_T^{NIN} in the absence of Andreev reflection ($\Delta_0 = 0$) aligns with the Δ_T^{NIN} result without spin-flip scattering in a NIN junction, as shown in Ref. [17]. It acts as a consistency check of our work. Furthermore, the ratio $\Delta_{Tsh}^{NIN}/\Delta_{Tth}^{NIN}$ in our work for a NIN junction ($\Delta_0 = 0$) is in agreement with ratio $\Delta_{Tsh}^{NIN}/\Delta_{Tth}^{NIN}$ given in Ref. [17] for a NIN junction.

A. Leading order contributions to Δ_{Tsh} and Δ_{Tth} noise

Here, we investigate the dominant order contributions from temperature difference to Δ_T noise, particularly focusing on Δ_{Tsh} and Δ_{Tth} noise. For the Δ_{Tsh}^{NIS} noise, the leading order contribution is from $(\Delta T)^2$ term, see Eq. (8). Likewise, for Δ_{Tth}^{NIS} noise, the leading order contribution from the temperature gradient is quadratic, i.e., $(\Delta T)^2$ (see, Eq. (9)). However, it is to be noted that there is a term independent of temperature difference (ΔT) in Δ_{Tth} noise, see Eq. (9). Consequently, for Δ_T noise, the leading order contribution also arises from $(\Delta T)^2$, stemming from both Δ_{Tsh} and Δ_{Tth} noise, as $\Delta_{Tsh(th)}$ noise shows a quadratic dependence on $(\Delta T)^2$ in NIS junction. Again, because of the term independent of temperature difference (ΔT) in Δ_{Tth} noise, there is consequently a term independent of ΔT in total Δ_T noise. Similarly, leading order contribution to total Δ_{Tsh}^{NIN} noise is from $(\Delta T)^2$ in a NIN junction. There is a term independent of ΔT in Δ_{Tth}^{NIN} noise, thus, leads to a term independent of ΔT in total Δ_{Tsh}^{NIN} noise, see Eq. (9). These dependencies are also observed in previous work [6]. It serves to ensure the consistency of our work.

Measurement of the total Δ_T noise as a function of temperature difference discerns the temperature-dependent behavior of Δ_{Tth} noise, which is the dominant contribution to Δ_T noise [6, 9]. In Table I, we present a summary of the leading

Table I. Leading order contributions from temperature difference (ΔT) to Δ_{Tsh}^η and Δ_{Tth}^η noise. [†] There is a term independent of temperature difference (ΔT) in Δ_{Tth}^η noise, see Eq. (9).

	Δ_{Tsh}^η	Δ_{Tth}^η
NIS	$\propto \Delta T^2$	$\propto \Delta T^2$
NIN	$\propto \Delta T^2$	$\propto \Delta T^2$

order contributions stemming from the temperature difference (ΔT) term to Δ_{Tsh}^η and Δ_{Tth}^η noise, where $\eta = NIS$ for NIS junction and $\eta = NIN$ for a NIN junction.

IV. ANALYSIS

In Table II, we summarize the ratio of $\Delta_T^{NIS}/\Delta_T^{NIN}$, along with the ratios of $\Delta_{Tsh}^{NIS}/\Delta_{Tsh}^{NIN}$ and $\Delta_{Tth}^{NIS}/\Delta_{Tth}^{NIN}$ for various regimes of barrier strength Z .

Table II. Ratio of $\Delta_T^{NIS}/\Delta_T^{NIN}$, along with the ratios of $\Delta_{Tsh}^{NIS}/\Delta_{Tsh}^{NIN}$ and $\Delta_{Tth}^{NIS}/\Delta_{Tth}^{NIN}$, for different regimes of barrier strength Z : transparent limit ($Z \rightarrow 0$), intermediate limit ($Z \rightarrow 1$) and tunnel limit ($Z \rightarrow \text{large}$).

	Transparent limit $Z \rightarrow 0$	Intermediate limit $Z \rightarrow 1$	Tunnel limit $Z \rightarrow \text{large}$
$\frac{\Delta_T^{NIS}}{\Delta_T^{NIN}}$	≈ 2	$\approx 3/2$	≈ 1
$\frac{\Delta_{Tsh}^{NIS}}{\Delta_{Tsh}^{NIN}}$	≈ 2	$\approx 3/2$	≈ 1
$\frac{\Delta_{Tth}^{NIS}}{\Delta_{Tth}^{NIN}}$	≈ 2	≈ 2	≈ 1

In the transparent limit, when Z is small, the Δ_T noise remains

finite, primarily due to Δ_T thermal-noise, the dominant contribution for both NIS and NIN junctions. Interestingly, in the transparent limit, Δ_T^{NIS} noise is double the value of Δ_T^{NIN} noise, i.e., $\Delta_T^{NIS}/\Delta_T^{NIN} \approx 2$. Both Δ_T thermal and Δ_T shot-noise in the NIS junction are nearly twice the magnitude of those in the NIN junction. It is solely due to the perfect Andreev reflection in the transparent limit for a NIS junction. As the barrier strength increases, the ratio $\Delta_T^{NIS}/\Delta_T^{NIN}$ decreases in the intermediate limit ($Z \rightarrow 1$). The ratio $\Delta_{Tsh}^{NIS}/\Delta_{Tsh}^{NIN}$ decreases at a slower rate compared to the ratio $\Delta_{Tth}^{NIS}/\Delta_{Tth}^{NIN}$. However, in the tunnel limit ($Z \rightarrow \text{large}$), the Δ_T noise in a NIS junction tends towards the same value as the Δ_T noise in a NIN junction.

In a recent work [13], the authors investigated the temperature gradient generated quantum noise in a metal/superconductor junction to examine the influence of the superconductor on transport phenomena in comparison to a metal/metal junction in zero voltage case ($V_1 = V_2 = 0$). The study revealed that the temperature gradient generated by quantum noise in the metal/superconductor junction is amplified compared to the metal/metal junction as a temperature gradient function. Furthermore, temperature gradient generated quantum noise is calculated in two limits: transparent limit and intermediate barrier strength limit in a NIS junction. They find that the temperature gradient generated by quantum noise is sensitive to interface strength [13]. However, they did not delve into the discussion of Δ_T thermal-noise contribution and Δ_T shot-noise contribution.

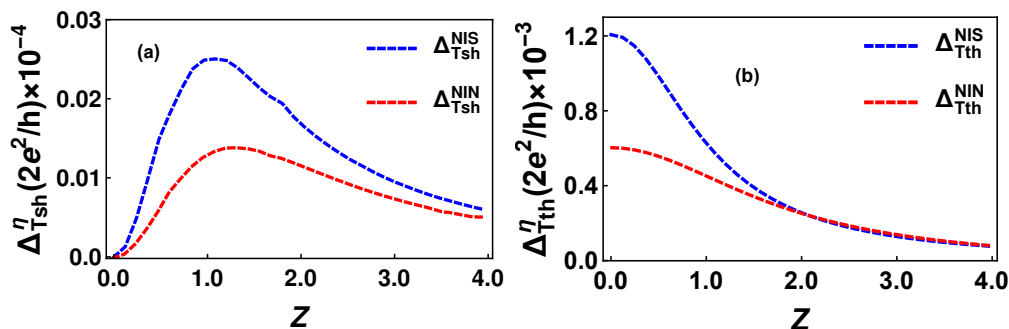


Figure 4. (a) Δ_{Tsh}^η , and (b) Δ_{Tth}^η noise vs. Z with $\frac{\Delta_T}{2T} = 0.14$ and $\eta \in \{NIS, NIN\}$.

In Fig. 4, we plot Δ_{Tsh}^η and Δ_{Tth}^η noise as functions of the barrier strength Z for our chosen setup, see Fig. 1. For intermediate barrier strength, Δ_{Tsh}^{NIS} exhibits a distinct sharp peak, primarily attributed to the contributions from Andreev reflection and normal reflection in a NIS junction. Similarly, Δ_{Tsh}^{NIN} noise also shows a peak at almost the same Z value in a NIN junction, albeit with a lower magnitude compared to the Δ_{Tsh}^{NIS} noise in a NIS junction. Δ_{Tth}^η noise is always higher than Δ_{Tsh}^η noise and shows a peak in the transparent limit and gradually decreases as Z increases for both NIS and NIN junctions. Im-

portantly, Andreev reflection plays a pivotal role in enhancing Δ_{Tth}^η noise, especially in the transparent limit, consequently leading to an increase in Δ_T noise in NIS junction (see Fig. 3). In the tunnel limit, both Δ_{Tsh}^{NIN} and Δ_{Tth}^{NIN} vanish, and Δ_{Tsh}^{NIS} and Δ_{Tth}^{NIS} also behave similarly to that of a NIN junction. Next, we explain the characteristics of Δ_{Tsh} shot-noise and Δ_{Tth} thermal-noise due to the Andreev reflection and normal reflection in both transparent and tunnel limits.

A. Transparent limit ($Z \rightarrow 0$)

In the transparent limit, for small barrier strength ($Z \rightarrow 0$), Andreev reflection probability $A \rightarrow 1$ below the superconducting gap ($E < \Delta_0$) while Andreev reflection probability decreases with energy above the superconducting gap ($E > \Delta_0$). In the transparent limit, normal reflection probability $B \rightarrow 0$ for both below and above the superconducting gap. Thus, Δ_{Tsh} shot noise contribution in a NIS junction, which depends on the scattering term $F_{11sh}^{NIS} = A(1-A) + B(1-B) + 2AB$ (see, Eq. (8)) vanishes in the transparent limit ($Z \rightarrow 0$).

In the transparent ($Z \rightarrow 0$) limit, Δ_{Tth}^{NIS} thermal-noise contribution to Δ_T^{NIS} noise depends on scattering term $F_{11th}^{NIS} = 1 + A - B$ (see, Eq. (9)) remains finite. It is due to the finite Andreev reflection probability $A \rightarrow 1$ below the gap $E < \Delta_0$, while normal reflection probability $B \rightarrow 0$. In the transparent limit, the ratio $\Delta_{Tsh}/\Delta_{Tth}$ vanishes for both NIS and NIN junctions due to vanishing Δ_{Tsh} shot-noise.

B. Intermediate ($Z \rightarrow 1$) and tunnel limit ($Z \rightarrow \text{large}$)

As barrier strength Z increases, Andreev reflection probability A increases with energy below the superconducting gap $E < \Delta_0$, while A decreases with energy above the superconducting gap $E > \Delta_0$. On the contrary, normal reflection proba-

bility B decreases with energy below the superconducting gap ($E < \Delta_0$) and increases above the gap. Thus, Δ_{Tsh} shot-noise contribution in a NIS junction which depends on scattering term $F_{11sh}^{NIS} = A(1-A) + B(1-B) + 2AB$ (see, Eq. (8)) shows a peak for intermediate barrier strength, see Fig. 4(a). Δ_{Tth} thermal-noise contribution in a NIS junction which depends on scattering term $F_{11th}^{NIS} = 1 + A - B$ (see, Eq. (9)) decreases for intermediate barrier strength due to decreasing A and increasing B with increase in value of Z , see Fig. 4(b).

As barrier strength Z increases beyond intermediate limit ($Z \rightarrow \text{large}$), the ratio $\Delta_{Tsh}/\Delta_{Tth}$ remains finite. In the tunnel limit ($Z \rightarrow \text{large}$), Andreev reflection probability $A \rightarrow 0$, while normal reflection probability $B \rightarrow 1$, for both below and above the superconducting gap. Thus, Δ_{Tsh} shot-noise and Δ_{Tth} thermal-noise contributions in a NIS junction vanish as $A \rightarrow 0$ and $B \rightarrow 1$ in the tunnel limit, see Figs. 4(a) and 4(b).

C. Quantum shot-noise (S_{11sh}) and thermal-noise (S_{11th})

In this subsection, we discuss the characteristics of finite temperature quantum noise (S_{11}), along with its contributions from shot-noise (S_{11sh}) and thermal-noise (S_{11th}) as a function of barrier strength Z with $\Delta_0 = 1.39\text{meV}$ and $E_F = 100\Delta_0$ in a NIS junction.

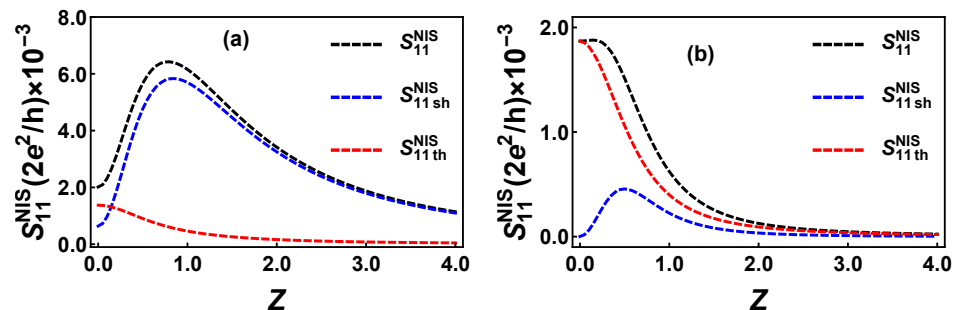


Figure 5. (Black) Quantum noise, (Red) thermal noise and (Blue) shot noise vs. Z , where $T_1 = T_2 = 4\text{K}$, with (a) $e\Delta V$ ($= 10\text{meV}$) $> k_B\bar{T}$, and (b) $e\Delta V$ ($= 0.02\text{meV}$) $< k_B\bar{T}$.

In Fig. 5, we plot total quantum noise, thermal-noise, and shot-noise vs. barrier strength Z at finite temperature $T_1 = T_2 = T$ and at finite voltage bias. For low-temperatures (see, Fig. 5 (a)), shot-noise dominates thermal-noise contribution as $e\Delta V \gg k_B\bar{T}$, i.e., $e\Delta V (= eV_1 - eV_2) = 10\text{meV}$ is larger than $k_B\bar{T} = 0.34\text{meV}$. However, for low voltage bias (see, Fig. 5 (b)), thermal-noise dominates shot-noise contribution as $e\Delta V \ll k_B\bar{T}$, where $e\Delta V = 0.02\text{meV}$, which is smaller than $k_B\bar{T} = 0.34\text{meV}$. As predicted before [2], quantum thermal-noise dominates quantum shot-noise contribution as $e\Delta V \ll k_B\bar{T}$ for low bias voltage case, and quantum shot-noise dom-

inates quantum thermal-noise contribution as $e\Delta V \gg k_B\bar{T}$ in low-temperatures for intermediate ($Z \rightarrow 1$) and tunnel limit ($Z \rightarrow \text{large}$). Nevertheless, in the transparent limit, characterized by perfect Andreev reflection and the vanishing normal reflection, shot-noise diminishes, and thermal-noise is finite. In contrast to quantum noise, Δ_T noise always obeys the general bound, i.e., $\Delta_{Tsh}/\Delta_{Tth} \leq 1$ and Δ_{Tth} set the upper bound limit regardless of the temperature and voltage bias configurations.

In Table III, we compare Δ_T^{NIS} noise with quantum noise (S_{11}^{NIS}) in a NIS junction. Δ_T^{NIS} noise always obeys the general

Table III. Comparison of Δ_T^{NIS} noise with quantum noise (S_{11}^{NIS}) in a NIS junction.

	Δ_T^{NIS} noise	Quantum noise (S_{11}^{NIS})
Dominant contribution	Δ_{Tth}^{NIS} thermal noise (see, Fig. 4)	S_{11sh}^{NIS} (for $e\Delta V > k_B\bar{T}$) (see, Fig. 5(a))
		S_{11th}^{NIS} (for $e\Delta V < k_B\bar{T}$) (see, Fig. 5(b))
General bound	$\Delta_{Tsh}^{NIS}/\Delta_{Tth}^{NIS} < 1$ (see, Fig. 3(b))	$S_{11sh}^{NIS}/S_{11th}^{NIS} > 1$ (for $e\Delta V > k_B\bar{T}$) (see, Fig. 5(a))
		$S_{11sh}^{NIS}/S_{11th}^{NIS} < 1$ (for $e\Delta V < k_B\bar{T}$) (see, Fig. 5(b))

bound, i.e., Δ_T^{NIS} thermal-noise is always greater than Δ_T^{NIS} shot-noise. On the contrary, quantum shot-noise S_{11sh}^{NIS} dominates quantum thermal-noise S_{11th}^{NIS} (see, Fig. 5(a)) for larger bias voltage, i.e., $e\Delta V > k_B\bar{T}$, breaking the general bound. However, quantum thermal-noise S_{11th}^{NIS} dominates quantum shot-noise S_{11sh}^{NIS} in low bias voltage limit (see, Fig. 5(b)), i.e., $e\Delta V < k_B\bar{T}$.

V. EXPERIMENTAL REALIZATION AND CONCLUSION

In recent studies, Δ_T noise has been measured due to a finite temperature difference, alongside its Δ_T thermal and Δ_T shot-noise contributions [9–11]. The procedure for determining the Δ_T shot-noise contribution involved subtracting the Δ_T thermal-noise component from the total Δ_T noise [9]. In Ref. [9], total Δ_T noise is measured in an atomic-scale molecular junction due to a finite temperature gradient at zero bias voltage. In our setup, we have a metal/insulator/s wave superconductor junction. One can choose the *s* wave superconductor, Niobium (Nb), with a superconducting gap $\Delta_0 = 1.39$ meV [15].

To design a NIS junction, a thin copper (Cu) film can be deposited (sputtered or patterned via lithography) on a niobium (Nb) superconductor base, which can be a suitable clean Normal metal/Superconductor sample [20]. To create an insulating barrier between the metal and the superconductor, the metal surface can be oxidized by ion beam lithography [21]. To measure Δ_T noise, the normal metal is connected to a heated diffusive wire, such that the normal metal is at a higher temperature than the superconductor. A finite current passes through the wire to control its temperature, thereby maintaining a temperature difference between both junction contacts, as mentioned in Ref. [11]. The current is applied only to the heated wire, while no current is applied in the junction, ensuring that no charge current but a pure heat current flows through the junction, isolating Δ_T noise solely due to the temperature

difference [11]. This experimental technique can measure Δ_T noise in a Normal/Insulator/Superconductor junction.

Here, our investigation delves into the behavior of Δ_T noise, explicitly focusing on the contributions from Δ_{Tsh} shot and Δ_{Tth} thermal-noise. We explore how these contributions vary with the barrier strength in the context of NIS (Normal/Insulator/Superconductor) and NIN (Normal/Insulator/Normal) junctions. In a NIS junction, the Δ_T thermal-noise (Δ_{Tth}) is the dominant contribution and is notably heightened compared to that in a NIN junction; this is especially evident in the transparent limit. This Δ_{Tth} noise behavior stems from perfect Andreev reflection and subsequent reduction in normal reflection. The Δ_T^{NIS} shot-noise (Δ_{Tsh}^{NIS}) vanishes in the transparent limit but shows a peak at intermediate barrier strength, attributed to contributions from both normal and Andreev reflections. However, as the barrier strength (Z) increases to the tunnel limit, both Δ_{Tth} and Δ_{Tsh} noise gradually vanish.

Similarly, in a NIN junction, Δ_{Tsh} noise peaks at intermediate barrier strength due to finite transmission probability. In a NIN junction, Δ_{Tsh} noise vanishes in the transparent limit, while Δ_{Tth} noise remains finite, resulting in non-zero Δ_T noise. Notably, Andreev reflection significantly amplifies Δ_T noise in a NIS junction compared to a NIN junction in the transparent limit.

We find the general bound for Δ_T noise in both NIS (Normal/Insulator/Superconductor) and NIN (Normal/Insulator/Normal) junctions, wherein Δ_T shot-noise (Δ_{Tsh}) is consistently less than Δ_T thermal-noise (Δ_{Tth}). The ratio $\Delta_{Tsh}/\Delta_{Tth}$ consistently decreases in the transparent limit for both NIS and NIN junctions due to the negligible Δ_{Tsh} noise. Notably, Δ_T noise, along with both Δ_{Tsh} shot and Δ_{Tth} thermal-noise contributions, are sensitive to changes in barrier strength. This investigation provides valuable insights into the distinct characteristics of Δ_T noise, specifically the Δ_T shot-noise and Δ_T thermal-noise contributions. It also offers a deeper understanding of the interplay between temperature gradient and barrier strength in shaping the Δ_T noise behavior.

APPENDIX

The Appendix is divided into four sections. First, in Appendix A, we calculate the charge current in normal metal contact. Subsequently, we derive the quantum noise autocorrelation in Appendix B. Next, in Appendix C1, we calculate the charge thermovoltage after imposing the condition of vanishing charge current, which is needed to calculate Δ_T noise. In Appendix C2, we derive the Δ_T shot-noise and Δ_T thermal-noise contributions to Δ_T noise in NIS and NIN junctions, respectively.

Appendix A: Average current with finite temperature gradient

The average current ($\langle I_1 \rangle$) in the normal metal contact ($i = 1$) is,

$$\langle I_1 \rangle = \frac{e}{h} \sum_{\substack{k,l \in \{1,2\}, \\ \rho, \Gamma, \eta \in \{e,h\}}} sgn(\rho) \int_{-\infty}^{\infty} dE A_{k\Gamma;l\eta}(1\rho, E) \langle a_{k\Gamma}^{\dagger}(E) a_{l\eta}(E) \rangle, \quad (\text{A1})$$

where $A_{k\Gamma;l\eta}(1\rho, E) = \delta_{1k}\delta_{1l}\delta_{\rho\Gamma}\delta_{\rho\eta} - s_{1k}^{\rho\Gamma\dagger} s_{1l}^{\rho\eta}$. The expectation value of $a_{k\Gamma}^{\dagger}(E) a_{l\eta}(E) \neq 0$ only when $k = l$ and $\Gamma = \eta$ and it is denoted as Fermi function in contact k for particle Γ (see Ref. [16]), i.e., $\langle a_{k\Gamma}^{\dagger}(E) a_{l\eta}(E) \rangle = \delta_{kl}\delta_{\Gamma\eta}f_{k\Gamma}(E) = f_{l\eta}(E)$. Fermi function in contact $k \in \{1, 2\}$, for particle $\Gamma \in \{e, h\}$ is $f_{k\Gamma}(E) = \left[1 + e^{\frac{E+sgn(\Gamma)V_k}{k_B T_k}}\right]^{-1}$, and $sgn(\rho) = sgn(\Gamma) = sgn(\eta) = +1$ for electron and -1 for hole. Thus, current in normal metal given in Eq. (A1) can be further simplified as:

$$\begin{aligned} \langle I_1 \rangle &= \frac{e}{h} \int_{-\infty}^{\infty} \sum_{\substack{k,l \in \{1,2\}, \\ \rho, \Gamma, \eta \in \{e,h\}}} sgn(\rho) \delta_{kl} \delta_{\Gamma\eta} f_{k\Gamma} A_{k\Gamma;l\eta}(1\rho, E) dE = \frac{e}{h} \int_{-\infty}^{\infty} \sum_{\substack{l \in \{1,2\}, \\ \rho, \eta \in \{e,h\}}} sgn(\rho) A_{l\eta;l\eta}(1\rho, E) f_{l\eta} dE \\ &= \frac{e}{h} \int_{-\infty}^{\infty} \sum_{\substack{l \in \{1,2\}, \\ \rho, \eta \in \{e,h\}}} sgn(\rho) (\delta_{1l}\delta_{\rho\eta} - |s_{1l}^{\rho\eta}|^2) f_{l\eta} dE. \end{aligned} \quad (\text{A2})$$

Fermi function of electron-like and hole-like quasiparticles in the superconductor can be expressed as $f_{2e} = \left(1 + e^{\frac{E-V_2}{k_B T_2}}\right)^{-1}$ and $f_{2h} = \left(1 + e^{\frac{E+V_2}{k_B T_2}}\right)^{-1}$ [2, 16]. Similarly, for the normal metal, the Fermi functions for electron and hole are given as $f_{1e} = \left(1 + e^{\frac{E-V_1}{k_B T_1}}\right)^{-1}$ and $f_{1h} = \left(1 + e^{\frac{E+V_1}{k_B T_1}}\right)^{-1}$. Using the properties $f_{1e}(-E) = 1 - f_{1h}(E)$, and $f_{2e}(-E) = 1 - f_{2h}(E)$, we get the average current in normal metal (see, Refs. [14, 18]) as follows,

$$\langle I_1 \rangle = \frac{2e}{h} \int_{-\infty}^{\infty} (1 + |s_{11}^{he}|^2 - |s_{11}^{ee}|^2) (f_{1e} - f_{2e}) dE = \frac{e}{h} \int_{-\infty}^{\infty} F_I^{NIS} (f_{1e}(E) - f_{2e}(E)) dE, \quad (\text{A3})$$

where $F_I^{NIS} = 1 + A - B$, with $A = |s_{11}^{he}|^2$ being the Andreev reflection probability and $B = |s_{11}^{ee}|^2$ is the normal reflection probability. To obtain the simplified current expression as given in Eq. (A3), we have used the properties $A(-E) = A$, and $B(-E) = B$ [2, 14, 18], along with the properties of probability conservation, i.e., $A + B + C + D = 1$, where C and D denote electron-like and hole-like transmission probabilities.

For a NIN junction, average current is $I_1^{NIN} = \frac{e}{h} \int_{-\infty}^{\infty} dE \mathcal{T} (f_{1e} - f_{2e}) = \frac{e}{h} \int_{-\infty}^{\infty} dE F_I^{NIN} (f_{1e} - f_{2e})$, where $F_I^{NIN} = \mathcal{T}$, where \mathcal{T} is the transmission probability, which aligns with I_1^{NIN} calculation given in Ref. [17].

Appendix B: Quantum noise

The current-current correlation [2, 3] between contacts p and q is defined $S_{pq}(t - t') = \frac{1}{2\pi} \langle \Delta I_p(t) \Delta I_q(t') + \Delta I_q(t') \Delta I_p(t) \rangle$, with $\Delta I_p = I_p - \langle I_p \rangle$, where I_p is current in lead p . Upon Fourier transforming the quantum noise, we obtain the quantum noise power, expressed in terms of frequency as $2\pi\delta(\omega + \bar{\omega})S_{pq}(\omega) \equiv \langle \Delta I_p(\omega) \Delta I_q(\bar{\omega}) + \Delta I_q(\bar{\omega}) \Delta I_p(\omega) \rangle$. Quantum noise at zero frequency $S_{pq}(\omega = \bar{\omega} = 0)$ [16], in a NIS junction is given as,

$$S_{pq}^{NIS} = \frac{2e^2}{h} \int \sum_{\substack{k,l \in \{1,2\}, \\ x,y,\Gamma,\eta \in \{e,h\}}} sgn(y) sgn(x) A_{l,\eta;k,\Gamma}(qy, E) A_{k,\Gamma;l,\eta}(px, E) f_{k\Gamma}(E) [1 - f_{l\eta}(E)] dE, \quad (\text{B1})$$

where $A_{k,\Gamma;l,\eta}(px, E) = \delta_{pk}\delta_{pl}\delta_{x\Gamma}\delta_{x\eta} - s_{pk}^{x\Gamma*}(E)s_{pl}^{x\eta}(E)$. Here $sgn(x) = sgn(y) = +1$ for electron and $sgn(x) = sgn(y) = -1$ for hole. Noise auto-correlation (i.e., $p = q = 1$), i.e., quantum noise in the normal metal of a NIS junction, is,

$$S_{11}^{NIS} = \frac{2e^2}{h} \int \sum_{\substack{k,l \in \{1,2\}, \\ x,y,\Gamma,\eta \in \{e,h\}}} sgn(y) sgn(x) A_{l,\eta;k,\Gamma}(1y, E) A_{k,\Gamma;l,\eta}(1x, E) f_{k\Gamma}(E) [1 - f_{l\eta}(E)] dE. \quad (B2)$$

Considering both electron and hole, quantum noise auto-correlation (S_{11}^{NIS}) can be separated as current-current correlations of the same particles (S_{11}^{sa}) and current-current correlations of different particles (S_{11}^{op}), i.e., $S_{11} = S_{11}^{sa} + S_{11}^{op}$, see Ref. [16], where $S_{11}^{sa} = \langle \Delta\hat{I}_{1e}\Delta\hat{I}_{1e} + \Delta\hat{I}_{1h}\Delta\hat{I}_{1h} \rangle$, and $S_{11}^{op} = \langle \Delta\hat{I}_{1e}\Delta\hat{I}_{1h} + \Delta\hat{I}_{1h}\Delta\hat{I}_{1e} \rangle$, given as,

$$\begin{aligned} S_{11}^{sa} &= \frac{2e^2}{h} \int \sum_{\substack{k,l \in \{1,2\}, \\ x,y,\Gamma,\eta \in \{e,h\}}} A_{k,\Gamma;l,\eta}(1x, E) A_{l,\eta;k,\Gamma}(1x, E) f_{k\Gamma}(E) [1 - f_{l\eta}(E)] dE \\ &= \frac{2e^2}{h} \int \sum_{\substack{k,l \in \{1,2\}, \\ x,y,\Gamma,\eta \in \{e,h\}}} \left[(1 - T_{11}^{xx})^2 f_{1x}(1 - f_{1x}) + \sum_{\substack{k \neq 1; l \neq 1; \\ \Gamma \neq x; \eta \neq x}} T_{1k}^{x\Gamma} T_{1l}^{x\eta} f_{k\Gamma}(1 - f_{l\eta}) \right] dE \\ S_{11}^{op} &= -\frac{2e^2}{h} \int \sum_{\substack{k,l \in \{1,2\}, \\ x,y,\Gamma,\eta \in \{e,h\}, x \neq y}} A_{k,\Gamma;l,\eta}(1x, E) A_{l,\eta;k,\Gamma}(1y, E) f_{k\Gamma}(E) [1 - f_{l\eta}(E)] dE \\ &= \frac{2e^2}{h} \int \sum_{x \in \{e,h\}} \left[2T_{11}^{x\bar{x}} f_{1\bar{x}}(1 - f_{1\bar{x}}) + \sum_{\substack{k \in \{1,2\}; \\ \Gamma \in \{e,h\}}} S_{1k}^{x\Gamma} S_{1k}^{x\Gamma\dagger} f_{k\Gamma} \sum_{\substack{l \in \{1,2\}; \\ \eta \in \{e,h\}}} S_{1l}^{x\eta} S_{1l}^{x\eta\dagger} f_{l\eta} \right] dE. \end{aligned} \quad (B3)$$

To derive the simplified quantum noise expression, we utilize the properties $A(-E) = A$, and $B(-E) = B$ [2, 14, 19], where A and B are Andreev reflection and normal reflection probabilities along with the properties of probability conservation, i.e., $A + B + C + D = 1$, where C and D denote electron-like and hole-like transmission probabilities. Further, Fermi functions can be simplified using the properties $f_{1e}(-E) = 1 - f_{1h}(E)$, and $f_{2e}(-E) = 1 - f_{2h}(E)$ [2, 14, 18].

Thus, quantum noise auto-correlation can be simplified as,

$$\begin{aligned} S_{11}^{NIS} &= \frac{4e^2}{h} \int_{-\infty}^{\infty} \left[(1 + |s_{11}^{ee}|^2 |s_{11}^{ee}|^2 - 2|s_{11}^{ee}|^2 + |s_{11}^{he}|^2 |s_{11}^{he}|^2 - 2|s_{11}^{he}|^2 |s_{11}^{ee}|^2) (f_{1e}(1 - f_{1e}) + f_{2e}(1 - f_{2e})) \right. \\ &\quad \left. + (|s_{11}^{ee}|^2 (1 - |s_{11}^{ee}|^2) + |s_{11}^{he}|^2 (1 - |s_{11}^{he}|^2) + 2|s_{11}^{ee}|^2 |s_{11}^{he}|^2) (f_{1e}(1 - f_{2e}) + f_{2e}(1 - f_{1e})) \right] dE \\ &= \frac{4e^2}{h} \int_{-\infty}^{\infty} \left[((1 - B)^2 + A^2 - 2A B) (f_{1e}(1 - f_{1e}) + f_{2e}(1 - f_{2e})) + (B(1 - B) + A(1 - A) + 2AB) (f_{1e}(1 - f_{2e}) + f_{2e}(1 - f_{1e})) \right] dE \\ &= \frac{4e^2}{h} \int_{-\infty}^{\infty} \left[(1 + A - B) (f_{1e}(1 - f_{1e}) + f_{2e}(1 - f_{2e})) + (B(1 - B) + A(1 - A) + 2AB) (f_{1e} - f_{2e})^2 \right] dE, \end{aligned} \quad (B4)$$

where terms involving Fermi function coefficient $(f_{1e}(1 - f_{1e}) + f_{2e}(1 - f_{2e}))$ denoted as quantum thermal-noise that vanishes at zero temperature. On the other hand, the terms with $(f_{1e} - f_{2e})^2$ correspond to quantum shot-noise, which vanishes at zero bias voltage [13, 19, 22]. Shot-noise auto-correlation can be calculated from Eq. (B4) as,

$$S_{11sh}^{NIS} = \frac{4e^2}{h} \int_{-\infty}^{\infty} dE \left[(B(1 - B) + A(1 - A) + 2AB) (f_{1e} - f_{2e})^2 \right] = \frac{4e^2}{h} \int_{-\infty}^{\infty} F_{11sh}^{NIS} (f_{1e} - f_{2e})^2 dE, \quad (B5)$$

where $F_{11sh}^{NIS} = B(1 - B) + A(1 - A) + 2AB$. Thermal-noise auto-correlation is derived from Eq. (B4) as,

$$S_{11th}^{NIS} = \frac{4e^2}{h} \int_{-\infty}^{\infty} dE \left[(1 + A - B) (f_{1e}(1 - f_{1e}) + f_{2e}(1 - f_{2e})) \right] = \frac{4e^2}{h} \int_{-\infty}^{\infty} F_{11th}^{NIS} (f_{1e}(1 - f_{1e}) + f_{2e}(1 - f_{2e})) dE, \quad (B6)$$

where $F_{11th}^{NIS} = 1 + A - B$. Δ_T noise auto-correlations in a NIS junction has been studied in Ref. [13], which aligns with Eq.(B4). Total quantum noise in a NIN junction is $S_{11}^{NIN} = S_{11sh}^{NIN} + S_{11th}^{NIN}$, where the shot-noise contribution (S_{11sh}^{NIN}) and thermal-noise

contribution (S_{11th}^{NIN}) are given as,

$$S_{11sh}^{NIN} = \frac{2e^2}{h} \int_{-\infty}^{\infty} dE [\{\mathcal{T}(1-\mathcal{T})\} (f_{1e} - f_{2e})^2] = \frac{2e^2}{h} \int_{-\infty}^{\infty} F_{11sh}^{NIN} (f_{1e} - f_{2e})^2 dE,$$

$$\text{and } S_{11th}^{NIN} = \frac{2e^2}{h} \int_{-\infty}^{\infty} dE [\mathcal{T}(f_{1e}(1-f_{1e}) + f_{2e}(1-f_{2e}))] = \frac{2e^2}{h} \int_{-\infty}^{\infty} F_{11th}^{NIN} (f_{1e}(1-f_{1e}) + f_{2e}(1-f_{2e})) dE, \quad (B7)$$

where the scattering terms depend on the transmission probability \mathcal{T} , and $F_{11sh}^{NIN} = \mathcal{T}(1-\mathcal{T}) = |s_{21}^N|^2 (1-|s_{21}^N|^2)$ while $F_{11th}^{NIN} = \mathcal{T} = |s_{21}^N|^2$, which aligns with S_{11sh}^{NIN} shot-noise and S_{11th}^{NIN} thermal-noise calculations given in Ref. [17].

Appendix C: Thermovoltage V_{th} and Δ_T noise

1. Charge thermovoltage

Thermovoltage (V_{th}) is the applied voltage bias required to nullify the charge current in a NIS (NIN) junction to zero, tune it to zero [7], i.e., $\langle I_1^{NIS} (I_1^{NIN}) \rangle = 0$, see Appendix A for detailed derivation of charge current flowing in the NIS junction (see, Fig. 2). In our chosen setup, we have metal (N) and superconductor (S) contacts at comparable temperatures ($T_1 > T_2$), i.e., the temperature difference $\Delta T > 0$, but at zero bias voltage $\Delta V = 0$, i.e., both normal metal and superconductor are at same voltage bias ($V_1 = V_2 = V$). In our calculations, we assume the temperature difference ($\Delta T = T_1 - T_2$) is much smaller than the average temperature, $\bar{T} = (T_1 + T_2)/2$, i.e., $\frac{\Delta T}{2\bar{T}} \ll 1$. The Fermi functions for electrons in N and S contacts are given as $f_{1e} = \left[1 + e^{\frac{E-V}{k_B T_1}}\right]^{-1}$ and $f_{2e} = \left[1 + e^{\frac{E-V}{k_B T_2}}\right]^{-1}$, where $T_1 = \bar{T} + \frac{\Delta T}{2}$ and $T_2 = \bar{T} - \frac{\Delta T}{2}$. Thus, we can express $f_{1e}(T_1)$ as $f_{1e}(\bar{T} + \frac{\Delta T}{2})$ and $f_{2e}(T_2)$ as $f_{2e}(\bar{T} - \frac{\Delta T}{2})$.

To calculate the thermovoltage (V_{th}) in our chosen setup (see, Fig. 2), we employ a power series expansion in terms of $\frac{\Delta T}{2\bar{T}}$ for the Fermi functions occurring in current I_1 (see, Eq. (A3)) as follows,

$$f_{1e}(E, k_B T_1) - f_{2e}(E, k_B T_2) = 2k_B \bar{T} \frac{\partial f(E)}{\partial k_B \bar{T}} \left(\frac{\Delta T}{2\bar{T}}\right) + \frac{1}{3} (k_B \bar{T})^3 \frac{\partial^3 f(E)}{\partial (k_B \bar{T})^3} \left(\frac{\Delta T}{2\bar{T}}\right)^3 + O\left(\frac{\Delta T}{2\bar{T}}\right)^5, \quad (C1)$$

where $f(E) = 1/(1 + e^{\frac{E}{k_B \bar{T}}})$. To streamline the calculation of current and to maintain the accuracy of the outcomes, we adopt the approximation: $\frac{\Delta T}{2\bar{T}} \ll 1$, while neglecting the higher-order terms of $O\left(\frac{\Delta T}{2\bar{T}}\right)^5$. The average charge current in normal metal contact is, then,

$$\langle I_1^{NIS} \rangle = \frac{2e}{h} \int_{-\infty}^{\infty} F_I^{NIS} \left[2k_B \bar{T} \frac{\partial f(E)}{\partial k_B \bar{T}} \left(\frac{\Delta T}{2\bar{T}}\right) + \frac{1}{3} (k_B \bar{T})^3 \frac{\partial^3 f(E)}{\partial (k_B \bar{T})^3} \left(\frac{\Delta T}{2\bar{T}}\right)^3 \right] dE, \text{ where } F_I^{NIS} = 1 + A - B, \quad (C2)$$

where A and B are Andreev reflection and normal reflection probabilities.

The average charge current in normal metal contact in a NIN junction is, then,

$$\langle I_1^{NIN} \rangle = \frac{e}{h} \int_{-\infty}^{\infty} F_I^{NIN} \left[2k_B \bar{T} \frac{\partial f(E)}{\partial k_B \bar{T}} \left(\frac{\Delta T}{2\bar{T}}\right) + \frac{1}{3} (k_B \bar{T})^3 \frac{\partial^3 f(E)}{\partial (k_B \bar{T})^3} \left(\frac{\Delta T}{2\bar{T}}\right)^3 \right] dE, \text{ where } F_I^{NIN} = \mathcal{T}, \quad (C3)$$

where \mathcal{T} is the transmission probability.

We evaluate the integrals given in Eqs. (C2) - (C3) numerically and equate $\langle I_1^{NIS(NIN)} \rangle = 0$, to get the thermovoltage (V_{th}) in the NIS and NIN junctions.

2. Δ_T noise with shot noise (Δ_{Tsh}) and thermal-noise (Δ_{Tth}) contributions

Next, we calculate the Δ_T noise in our chosen setup for contacts at comparable temperatures ($T_1 > T_2$) at zero voltage bias ($V_1 = V_2 = V$), see Fig. 2. Fermi functions occurring in quantum noise (see, Eq. (B4)) for electron in normal metal contact (1) and superconductor contact (2) can be written as $f_{1e}(T_1) = f_{1e}(\bar{T} + \frac{\Delta T}{2})$, and $f_{2e}(T_2) = f_{2e}(\bar{T} - \frac{\Delta T}{2})$, as $T_1 = \bar{T} + \frac{\Delta T}{2}$, $T_2 = \bar{T} - \frac{\Delta T}{2}$.

The Δ_T noise is obtained from quantum noise, as indicated in Eq. (B4), in the limit $\frac{\Delta T}{2\bar{T}} \ll 1$. Additionally, we break Δ_T noise into two parts, which are Δ_T shot-noise and Δ_T thermal-noise, given as $\Delta_T = \Delta_{Tsh} + \Delta_{Tth}$. Quantum shot-noise from Eq. (B5)

given in Appendix B leads to Δ_{Tsh} shot-noise contribution to Δ_T noise. By expanding the Fermi functions in a power series of $\frac{\Delta T}{2T}$, we have Fermi functions occurring in the quantum shot-noise contribution (see, Eq. (B4)) to be:

$$\begin{aligned} (f_{1e}(k_B T_1) - f_{2e}(k_B T_2))^2 &= \left(2 \frac{\partial f(E)}{\partial k_B \bar{T}}\right)^2 \left(\frac{k_B \Delta T}{2}\right)^2 + \left(\frac{1}{3}\right)^2 \left(\frac{\partial^3 f(E)}{\partial (k_B \bar{T})^3}\right)^2 \left(\frac{k_B \Delta T}{2}\right)^6 + \frac{4}{3} \frac{\partial f(E)}{\partial k_B \bar{T}} \frac{\partial^3 f(E)}{\partial (k_B \bar{T})^3} \left(\frac{k_B \Delta T}{2}\right)^4 \\ &= \left(2k_B \bar{T} \frac{\partial f(E)}{\partial k_B \bar{T}}\right)^2 \left(\frac{\Delta T}{2\bar{T}}\right)^2 + \frac{4}{3} (k_B \bar{T})^4 \frac{\partial f(E)}{\partial k_B \bar{T}} \frac{\partial^3 f(E)}{\partial (k_B \bar{T})^3} \left(\frac{\Delta T}{2\bar{T}}\right)^4 + O\left(\frac{\Delta T}{2\bar{T}}\right)^6, \end{aligned} \quad (\text{C4})$$

where $f(E) = 1/(1 + e^{\frac{E}{k_B \bar{T}}})$.

In the limit $\frac{\Delta T}{2\bar{T}} \ll 1$, and including terms up to $\left(\frac{\Delta T}{2\bar{T}}\right)^4$, Δ_T shot-noise (Δ_{Tsh}) in a NIS junction can be written as,

$$\Delta_{Tsh}^{NIS} = \frac{4e^2}{h} \int_{-\infty}^{\infty} F_{11sh}^{NIS} \left[\left(2k_B \bar{T} \frac{\partial f(E)}{\partial k_B \bar{T}}\right)^2 \left(\frac{\Delta T}{2\bar{T}}\right)^2 + \frac{4}{3} (k_B \bar{T})^4 \frac{\partial f(E)}{\partial k_B \bar{T}} \frac{\partial^3 f(E)}{\partial (k_B \bar{T})^3} \left(\frac{\Delta T}{2\bar{T}}\right)^4 \right] dE, \quad (\text{C5})$$

where $F_{11sh}^{NIS} = A(1 - A) + B(1 - B) + 2AB$ is given in Eq. (B5). We evaluate the integral given in Eq. (C5) in Mathematica after replacing the voltage bias V with the thermovoltage (V_{th}) to derive the Δ_{Tsh} noise.

Similarly, quantum thermal-noise (S_{11th}) from Eq. (B6) given in Appendix B leads to Δ_{Tth} thermal-noise by applying a finite temperature difference at zero voltage bias. Fermi functions in the quantum thermal-noise expression (see, Eq. (B6)) can be expanded in power series of $\frac{\Delta T}{2\bar{T}}$, and the in the limit $\frac{\Delta T}{2\bar{T}} \ll 1$, are given as,

$$\begin{aligned} f_{1e}(k_B T_1) - f_{1e}(k_B T_1)^2 + f_{2e}(k_B T_2) - f_{2e}(k_B T_2)^2 &= -k_B T_1 \frac{\partial f_{1e}(k_B T_1)}{\partial E} - k_B T_2 \frac{\partial f_{2e}(k_B T_2)}{\partial E} \\ &= -2k_B \bar{T} \frac{\partial f(E)}{\partial E} - \frac{\partial}{\partial E} \left(\frac{\partial^2 k_B \bar{T} f(E)}{\partial (k_B \bar{T})^2} \right) \left(\frac{k_B \Delta T}{2}\right)^2 - \frac{1}{3} \frac{\partial}{\partial E} \left(\frac{\partial^3 f(E)}{\partial (k_B \bar{T})^3} + \frac{\partial^4 f(E)}{\partial (k_B \bar{T})^4} \frac{k_B \bar{T}}{4} \right) \left(\frac{k_B \Delta T}{2}\right)^4 + O\left(\frac{\Delta T}{2\bar{T}}\right)^6 \\ &= - \left[2k_B \bar{T} \frac{\partial f(E)}{\partial E} + (k_B \bar{T})^2 \left\{ 2 \frac{\partial}{\partial E} \left(\frac{\partial f(E)}{\partial k_B \bar{T}} \right) + k_B \bar{T} \frac{\partial}{\partial E} \left(\frac{\partial^2 f(E)}{\partial (k_B \bar{T})^2} \right) \right\} \left(\frac{\Delta T}{2\bar{T}}\right)^2 + \frac{1}{3} (k_B \bar{T})^4 \left\{ \frac{\partial}{\partial E} \left(\frac{\partial^3 f(E)}{\partial (k_B \bar{T})^3} \right) \right. \right. \\ &\quad \left. \left. + \frac{k_B \bar{T}}{4} \frac{\partial}{\partial E} \left(\frac{\partial^4 f(E)}{\partial (k_B \bar{T})^4} \right) \right\} \left(\frac{\Delta T}{2\bar{T}}\right)^4 \right]. \end{aligned} \quad (\text{C6})$$

The Δ_T thermal-noise (Δ_{Tth}) in a NIS junction can then be derived as,

$$\begin{aligned} \Delta_{Tth}^{NIS} &= \frac{4e^2}{h} \int_{-\infty}^{\infty} F_{11th}^{NIS} \left[-k_B T_1 \frac{\partial f_{1e}(E, k_B T_1)}{\partial E} - k_B T_2 \frac{\partial f_{2e}(E, k_B T_2)}{\partial E} \right] dE \\ &= -\frac{4e^2}{h} \int_{-\infty}^{\infty} F_{11th}^{NIS} \left[2k_B \bar{T} \frac{\partial f(E)}{\partial E} + (k_B \bar{T})^2 \left\{ 2 \frac{\partial}{\partial E} \left(\frac{\partial f(E)}{\partial k_B \bar{T}} \right) + \frac{\partial}{\partial E} \left(\frac{\partial^2 f(E)}{\partial (k_B \bar{T})^2} \right) k_B \bar{T} \right\} \left(\frac{\Delta T}{2\bar{T}}\right)^2 + \frac{1}{3} (k_B \bar{T})^4 \left\{ \frac{\partial}{\partial E} \left(\frac{\partial^3 f(E)}{\partial (k_B \bar{T})^3} \right) \right. \right. \\ &\quad \left. \left. + \frac{k_B \bar{T}}{4} \frac{\partial}{\partial E} \left(\frac{\partial^4 f(E)}{\partial (k_B \bar{T})^4} \right) \right\} \left(\frac{\Delta T}{2\bar{T}}\right)^4 \right] dE, \end{aligned} \quad (\text{C7})$$

where $F_{11th}^{NIS} = 1 + A - B$.

Similarly, in a NIN junction, the Δ_T^{NIN} shot-noise can be derived as,

$$\Delta_{Tsh}^{NIN} = \frac{2e^2}{h} \int_{-\infty}^{\infty} F_{11sh}^{NIN} \left[\left(2k_B \bar{T} \frac{\partial f(E)}{\partial k_B \bar{T}}\right)^2 \left(\frac{\Delta T}{2\bar{T}}\right)^2 + \frac{4}{3} (k_B \bar{T})^4 \left(\frac{\partial f(E)}{\partial k_B \bar{T}} \frac{\partial^3 f(E)}{\partial (k_B \bar{T})^3}\right) \left(\frac{\Delta T}{2\bar{T}}\right)^4 \right] dE, \quad (\text{C8})$$

where the scattering term $F_{11sh}^{NIN} = \mathcal{T}(1 - \mathcal{T})$.

Δ_T^{NIN} thermal-noise in a NIN junction can also be derived as,

$$\begin{aligned} \Delta_{Tth}^{NIN} &= -\frac{2e^2}{h} \int_{-\infty}^{\infty} F_{11th}^{NIN} \left[2k_B \bar{T} \frac{\partial f(E)}{\partial E} + (k_B \bar{T})^2 \left\{ 2 \frac{\partial}{\partial E} \left(\frac{\partial f(E)}{\partial k_B \bar{T}} \right) + \frac{\partial}{\partial E} \left(\frac{\partial^2 f(E)}{\partial (k_B \bar{T})^2} \right) k_B \bar{T} \right\} \left(\frac{\Delta T}{2\bar{T}}\right)^2 + \frac{1}{3} (k_B \bar{T})^4 \right. \\ &\quad \left. \left\{ \frac{\partial}{\partial E} \left(\frac{\partial^3 f(E)}{\partial (k_B \bar{T})^3} \right) + \frac{k_B \bar{T}}{4} \frac{\partial}{\partial E} \left(\frac{\partial^4 f(E)}{\partial (k_B \bar{T})^4} \right) \right\} \left(\frac{\Delta T}{2\bar{T}}\right)^4 \right] dE, \end{aligned} \quad (\text{C9})$$

with the scattering term $F_{11th}^{NIN} = \mathcal{T}$.

The integrals given in Eqs. (C5-C9) are calculated numerically using Mathematica to get Δ_T , Δ_{Tth} and Δ_{Tsh} noise.

[1] C. Beenakker and C. Schönenberger, Quantum Shot Noise, Phys. Today 56, 5, 37 (2003).

[2] Ya M. Blanter, and M. Büttiker, Shot Noise in Mesoscopic Conductors, Phys. Reports 336, 1 (2000).

[3] L. P. Kouwenhoven, G. Schön, and L.L. Sohn, Introduction to mesoscopic electron transport, NATO ASI Series E, Kluwer Academic Publishing, Dordrecht, 225, 345 (1997).

[4] M. Henny, et. al., The Fermionic Hanbury Brown and Twiss Experiment, Science 284, 296 (1999); T. Mohapatra, S. Pal, and C. Benjamin, Probing the topological character of superconductors via nonlocal Hanbury Brown and Twiss correlations, Phys. Rev. B 106, 125402 ()

[5] J. Rech, et. al., Negative Delta-T Noise in the Fractional Quantum Hall Effect, Phys. Rev. Lett. 125, 086801 (2020).

[6] A. Popoff, et. al., Scattering theory of non-equilibrium noise and delta T current fluctuations through a quantum dot, J. Phys.: Condens. Matter 34, 185301 (2022).

[7] J. Eriksson, et. al., General Bounds on Electronic Shot Noise in the Absence of Currents, Phys. Rev. Lett. 127, 136801 (2021).

[8] L. Tesser, et. al., Charge, spin, and heat shot noises in the absence of average currents: Conditions on bounds at zero and finite frequencies, Phys. Rev. B 107, 075409 (2023).

[9] O. S. Limbroso, et. al., Electronic noise due to temperature differences in atomic-scale junctions, Nature 562, 240 (2018).

[10] E. Sivre, et. al., Electronic heat flow and thermal shot noise in quantum circuits, Nat. Comm. 10, 5638 (2019).

[11] S. Larocque, et. al., Shot Noise of a Temperature-Biased Tunnel Junction, Phys. Rev. Lett. 125, 106801 (2020).

[12] G. Zhang, I. V. Gornyi and C. Spaanslatt, Delta-T noise for weak tunneling in one-dimensional systems: Interactions versus quantum statistics, Phys. Rev. B 105, 195423 (2022).

[13] E. Zhitlukhina, M. Belogolovskii, P. Seidel, Electronic noise generated by a temperature gradient across a hybrid normal metal–superconductor nanojunction, Applied Nanosci. 10, 5121 (2020).

[14] G. E. Blonder, M. Tinkham, and T. M. Klapwijk, Transition from metallic to tunneling regimes in superconducting microconstrictions: Excess current, charge imbalance, and supercurrent conversion, Phys. Rev. B 25, 4515 (1982).

[15] Piotr Magierski, Gabriel Wlazłowski, and Aurel Bulgac, Onset of a Pseudogap Regime in Ultracold Fermi Gases, Phys. Rev. Lett. 107, 145304 (2011).

[16] M. P. Anantram and S. Datta, Current fluctuations in mesoscopic systems with Andreev scattering, Phys. Rev. B 53, 16390 (1996).

[17] T. Mohapatra and C. Benjamin, Spin-flip scattering engendered negative Δ_T noise, arXiv:2307.14072 (2023).

[18] C. J. Lambert, Generalized Landauer formulae for quasiparticle transport in disordered superconductors, J. Phys.: Condens. Matter 3, 6579 (1991).

[19] T. Martin, Noise in mesoscopic physics, Les Houches Session LXXXI, H. Bouchiat et. al. eds. (Elsevier 2005).

[20] X. Jehl, M. Sanquer, R. Calemczuk, and D. Mailly, Detection of doubled shot noise in short normal-metal/superconductor junctions, Nature 405, 50 (2000).

[21] Jiasen Niu, et. al., Why Shot Noise Does Not Generally Detect Pairing in Mesoscopic Superconducting Tunnel Junctions, Phys. Rev. Lett. 132, 076001 (2024).

[22] G. B. Lesovik, T. Martin and J. Torres, Josephson frequency singularity in the noise of normal-metal–superconductor junctions, Phys. Rev. B 60, 11935 (1999).